

# Mitochondrial $\text{Ca}^{2+}$ uniporter (MCU)-dependent and MCU-independent $\text{Ca}^{2+}$ channels coexist in the inner mitochondrial membrane

Alexander I. Bondarenko · Claire Jean-Quartier · Warisara Parichatikanond · Muhammad Rizwan Alam · Markus Waldeck-Weiermair · Roland Malli · Wolfgang F. Graier

Received: 15 July 2013 / Revised: 10 October 2013 / Accepted: 12 October 2013 / Published online: 27 October 2013  
© The Author(s) 2013. This article is published with open access at Springerlink.com

**Abstract** A protein referred to as CCDC109A and then renamed to mitochondrial calcium uniporter (MCU) has recently been shown to accomplish mitochondrial  $\text{Ca}^{2+}$  uptake in different cell types. In this study, we investigated whole-mitoplast inward cation currents and single  $\text{Ca}^{2+}$  channel activities in mitoplasts prepared from stable MCU knockdown HeLa cells using the patch-clamp technique. In whole-mitoplast configuration, diminution of MCU considerably reduced inward  $\text{Ca}^{2+}$  and  $\text{Na}^{+}$  currents. This was accompanied by a decrease in occurrence of single channel activity of the intermediate conductance mitochondrial  $\text{Ca}^{2+}$  current (*i*-MCC). However, ablation of MCU yielded a compensatory 2.3-fold elevation in the occurrence of the extra large conductance mitochondrial  $\text{Ca}^{2+}$  current (*xl*-MCC), while the occurrence of bursting currents (*b*-MCC) remained unaltered. These data reveal *i*-MCC as MCU-dependent current while *xl*-MCC and *b*-MCC seem to be rather MCU-independent, thus, pointing to the engagement of at least two molecularly distinct mitochondrial  $\text{Ca}^{2+}$  channels.

**Keywords** Mitochondrial  $\text{Ca}^{2+}$  channels · Mitochondrial  $\text{Ca}^{2+}$  uniporter · MCU ·  $\text{Ca}^{2+}$  signaling

## Introduction

$\text{Ca}^{2+}$  uptake by mitochondria stimulates metabolic processes and can also initiate cell death pathways (for review, see [5, 8]).

Accordingly, mitochondrial  $\text{Ca}^{2+}$  channels represent promising molecular targets for future therapeutic modulation of mitochondria functions. A precise understanding of the molecular mechanisms of mitochondrial  $\text{Ca}^{2+}$  uptake, molecular structure, and function of mitochondrial  $\text{Ca}^{2+}$  channels is required. Therefore, identification and electrophysiological characterization of mitochondrial  $\text{Ca}^{2+}$  channels and especially pinpointing specific channel activity to specific proteins will provide invaluable insight into actual processes that accomplish mitochondrial  $\text{Ca}^{2+}$  uptake.

Although several proteins have been identified to contribute to mitochondrial  $\text{Ca}^{2+}$  uptake, such like the mitochondrial  $\text{Ca}^{2+}$  uptake 1 (MICU1) [18], uncoupling proteins 2 and 3 [22, 23], ryanodine receptors [20, 21], mitochondrial  $\text{Ca}^{2+}$  uniporter regulator 1 (MCUR1) [14], and the canonical transient receptor potential 3 channel [6], the mitochondrial  $\text{Ca}^{2+}$  uniporter, MCU, a transmembrane protein in the inner mitochondrial membrane, has been proposed to be dominantly responsible for mitochondrial  $\text{Ca}^{2+}$  uptake [1, 4]. Recent advancement of the patch-clamp approach using mitoplasts allowed to identify mitochondrial  $\text{Ca}^{2+}$  uniport as a highly  $\text{Ca}^{2+}$ -selective ion channel [13] that was dependent on the presence of MCU [3]. Moreover, MCU-established currents were sensitive to ruthenium red, which has been assumed to be a classic feature of the mitochondrial  $\text{Ca}^{2+}$  uniport. A point mutation in the putative pore domain of MCU decreased the sensitivity of the respective  $\text{Ca}^{2+}$  current to ruthenium red without changing the current magnitude [3]. However, integral  $\text{Ca}^{2+}$  currents through whole mitoplasts presented in the study of Chaudhuri et al. do not enable to discriminate between contributions of different single channel conductances [3]. Single channel recordings allowed to characterize more than one ruthenium red-sensitive  $\text{Ca}^{2+}$  inward current in mitoplasts isolated from cardiac myocytes

A. I. Bondarenko · C. Jean-Quartier · W. Parichatikanond · M. R. Alam · M. Waldeck-Weiermair · R. Malli · W. F. Graier (✉)  
Institute of Molecular Biology and Biochemistry, Center of Molecular Medicine, Medical University of Graz,  
Harrachgasse 21/III, 8010 Graz, Austria  
e-mail: wolfgang.graier@medunigraz.at

(mitochondrial  $\text{Ca}^{2+}$  currents 1 and 2; mCa1, mCa2) [17], mitochondrial ryanodine receptor channel activity [21], endothelial cells [small mitochondrial  $\text{Ca}^{2+}$  currents, intermediate mitochondrial  $\text{Ca}^{2+}$  currents (*i*-MCC), and large mitochondrial  $\text{Ca}^{2+}$  currents (*l*-MCC)] [9], and HeLa cells [*i*-MCC and the extra large mitochondrial  $\text{Ca}^{2+}$  current (*xl*-MCC)] [2, 9], thus challenging the concept of MCU being the one and only  $\text{Ca}^{2+}$  channel in the inner mitochondrial membrane. The present study was designed to characterize the impact of MCU knockdown on different  $\text{Ca}^{2+}$  currents in mitoplasts isolated from HeLa cells by applying electrophysiological recordings in whole-mitoplast and mitoplast-attached configurations. These experiments were complemented with fluorescent mitochondrial  $\text{Ca}^{2+}$  measurements in the respective wild type and MCU knockdown (MCU-KD) HeLa cells. We show that in divalent-free conditions,  $\text{Na}^+$  readily permeates ruthenium red (RuR)-sensitive  $\text{Ca}^{2+}$  channels and downregulation of MCU protein results in suppression of whole-mitoplast inward  $\text{Na}^+$  and  $\text{Ca}^{2+}$  currents and a decreased occurrence probability of *i*-MCC that was associated with a partial increase in occurrence of the *xl*-MCC [2].

## Materials and methods

Design and production of stably MCU knockdown HeLa cells and their corresponding control cells

HeLa MCU-KD and HeLa control cells have been produced upon request and supplied by TeBu-bio® (Tebu-bio SAS, Le Perray-en-Yvelines Cedex, France). HeLa cells with stable MCU knockdown and the respective scrambled control cells were produced by applying the SilenciX® technology (Tebu-bio, [www.tebu-bio.com](http://www.tebu-bio.com), Le Perray-en-Yvelines, France) using the following 5'-3' shRNA sequence against MCU: GGTGCAA TTTATCTTTATA.

Cell culture and isolation of mitochondria

All cells were grown on DMEM containing 10 % FCS, 50 U/ml penicillin, and 50  $\mu\text{g}/\text{ml}$  streptomycin. Mitochondria were freshly isolated as previously described [2]. Mitochondria were prepared from HeLa cells by differential centrifugation. Cells were trypsinized, harvested, and washed with PBS. The cell pellet was suspended in a 200-mM sucrose buffer containing 10 mM Tris-MOPS, 1 mM EGTA and protease inhibitor (1:50, P8340 Sigma, Vienna, Austria) (pH adjusted to 7.4 with TRIS), and homogenized with a glass-Teflon potter (40–50 strokes). Nuclear remnants and cell debris were centrifuged down at 900 g for 10 min. The supernatant was centrifuged at 3,000g for 20 min. The mitochondrial pellet was washed

and centrifuged down at 7,000g for 15 min. All fractions were kept on ice until further utilization.

## Preparation of mitoplasts

Isolation and preparation of mitoplasts (mitochondria devoid of outer membrane) from HeLa cells was performed as recently described [2]. Briefly, mitoplast formation was achieved by incubation of isolated mitochondria in hypotonic solution (5 mM HEPES, 5 mM sucrose, 1 mM EGTA, pH adjusted to 7.4 with KOH) for 8 min. Then, hypertonic solution (750 mM KCl, 80 mM HEPES, 1 mM EGTA, pH adjusted to 7.4 with KOH) was added to restore isotonicity.

## Mitoplast patch-clamp recordings

Single channel measurements were performed in the mitoplast-attached configuration as previously described [2, 9]. In brief, patch pipettes were pulled from glass capillaries using a Narishige puller (Narishige Co., Ltd., Tokyo, Japan), fire-polished, and had a resistance of 8–12 M $\Omega$ . Mitoplasts were bathed in the solution containing (in millimolars): 145 KCl, 1 EGTA, HEPES, and pH adjusted to 7.2 with KOH. For single channel recordings, the pipette solution contained 105 mM  $\text{CaCl}_2$  and 10 mM HEPES, 10  $\mu\text{M}$  cyclosporin A (Tocris Bioscience, Bristol, UK) and 10  $\mu\text{M}$  7-chloro-5-(2-chlorophenyl)-1,5-dihydro-4,1-benzothiazepin-2(3*H*)-one (CGP 37157, Ascent Scientific Ltd., Bristol, UK) to prevent opening of the permeability transition pore, and the activity of the mitochondrial  $\text{Na}^+/\text{Ca}^{2+}$  exchanger ( $\text{NCX}_{\text{mito}}$ ), respectively. pH was adjusted to 7.2 with  $\text{Ca}(\text{OH})_2$ . Single channel currents were recorded at a fixed holding potential indicated in the respective figures. For whole-mitoplast recordings, pipette solution contained (in millimolars): 120 Cs methanesulfonate, 30 CsCl, 1 EGTA, 110 sucrose, 2 gluconic acid, and pH by TEAOH to 7.2. For obtaining whole-mitoplast configuration, voltage steps of 300–600 mV and 20–50 ms duration were applied. Voltage ramps of 1 s duration from  $-160$  to  $+50$  mV were delivered every 5 or 10 s from the holding potential 0 mV. Currents were recorded using a patch-clamp amplifier (EPC7, List Electronics, Darmstadt, Germany). Data collection was performed using Clampex software of pClamp (V9.0, Molecular Devices, Sunnyvale, CA, USA). Signals obtained were low pass filtered at 1 kHz using an eight-pole Bessel filter (Frequency Devices) and digitized with a sample rate of 10 kHz using a Digidata 1200A A/D converter (Molecular Devices, Sunnyvale, CA, USA). All measurements were performed at room temperature. For recording cationic currents via whole mitoplasts, bath solution contained (in millimolars): 150 TRIS HCl, 1 EGTA, 1 EDTA, 10 HEPES with pH 7.2. For  $I_{\text{Na}}$  recording, NaCl was substituted for TRIS HCl.  $\text{Ca}^{2+}$ -containing bath solution for  $I_{\text{Ca}}$  recording

contained (in millimolars): 140 TRIS HCl, 3 CaCl<sub>2</sub>, 10 HEPES, and pH 7.2

#### Single cell Ca<sup>2+</sup> imaging and data acquisition

Imaging mitochondrial targeted cameleon 4mtD3cpv was performed on a digital wide field imaging system, the Till iMIC (Till Photonics Graefelfing, Germany) using a 40× objective (alpha Plan Fluor 40×, Zeiss, Göttingen, Germany). For illumination of the cameleon, an ultrafast switching monochromator, the Polychrome V (Till Photonics), was used for excitation light at 430 nm. Emission light was collected at 480 and 535 nm using a single beam splitter design (Dichrotome, Till Photonics). Images were recorded with a charged-coupled device camera (AVT Stringray F145B, Allied Vision Technologies, Stadtroda, Germany). For the data acquisition and the control of the digital fluorescence microscope, the live acquisition software version 2.0.0.12 (Till Photonics) was used. Experiments were performed at the same day than the isolation, purification, and electrophysiological measurements of the respective mitoplasts.

#### Experimental buffers for Ca<sup>2+</sup> measurements

Ca<sup>2+</sup> measurements in HeLa cells were performed by stimulating cells in Ca<sup>2+</sup>-containing environment. Cells were superfused by a Ca<sup>2+</sup>-containing buffer, which was composed of (in millimolars): 138 NaCl, 5 KCl, 2 CaCl<sub>2</sub>, 1 MgCl<sub>2</sub>, 10 D-glucose and 10 HEPES, and pH adjusted to 7.4 with NaOH. Stimulation was performed using 100 μM of the IP<sub>3</sub>-generating agonist histamine.

#### Western blot

HeLa cells that were washed with ice-cold PBS or isolated mitochondria were lysed with RIPA buffer containing protease inhibitor cocktail (Sigma-Aldrich, Vienna, Austria). The protein concentration was measured using the BCA protein assay (Thermo Fisher Scientific Inc., Vienna, Austria). Forty micrograms of protein were separated by SDS-PAGE and transferred to a nitrocellulose membrane. The membrane was incubated with the primary antibody at 4 °C overnight and the primary antigen-antibody complex was detected by incubating the blot with a horseradish peroxidase-conjugated secondary antibody at room temperature for 2 h. The membrane was further developed with the ECL Plus Western blotting detection system (GE Healthcare, Vienna, Austria). To control the equal amount of protein loading of whole cell lysates and isolated mitochondria, MCU expression (sc-246071; Santa Cruz, Vienna, Austria) were densitometrically normalized to β-actin (sc-47778; Santa Cruz) and VDAC (sc-32063 and sc-32059; Santa Cruz), respectively.

#### Real-time PCR

RNA was isolated from HeLa cells using a Total RNA isolation kit (PEQLAB Biotechnologie GmbH, Erlangen, Germany), and it was reverse transcribed using a High Capacity cDNA Reverse Transcription Kit (Applied Biosystems, USA). The analysis of the expression of the target genes was performed by conventional polymerase chain reaction (PCR) using GoTaq Green master mix (Promega, Madison, WI, USA) and real-time PCR using QuantiFast SYBR Green RT-PCR kit (Qiagen, Hilden, Germany) on LightCycler 480 (Roche Diagnostics, Vienna, Austria). RNA polymerase II (RPOL2) was used as a housekeeping control [12, 16, 24]. Primers for RPOL2 and MCU were obtained from Invitrogen (Vienna, Austria) and their sequences (5′–3′) were as follows: RPOL2: CATTGACTTGCGTTTCCACC, RPOL2 rev: ACATTTTGTGCAGAGTTGGC, MCU: TTCCTGGCAGAATTTGGGAG, and MCU rev: AGAGATAGGCTTGAGTGTGAAC.

#### Statistical analysis

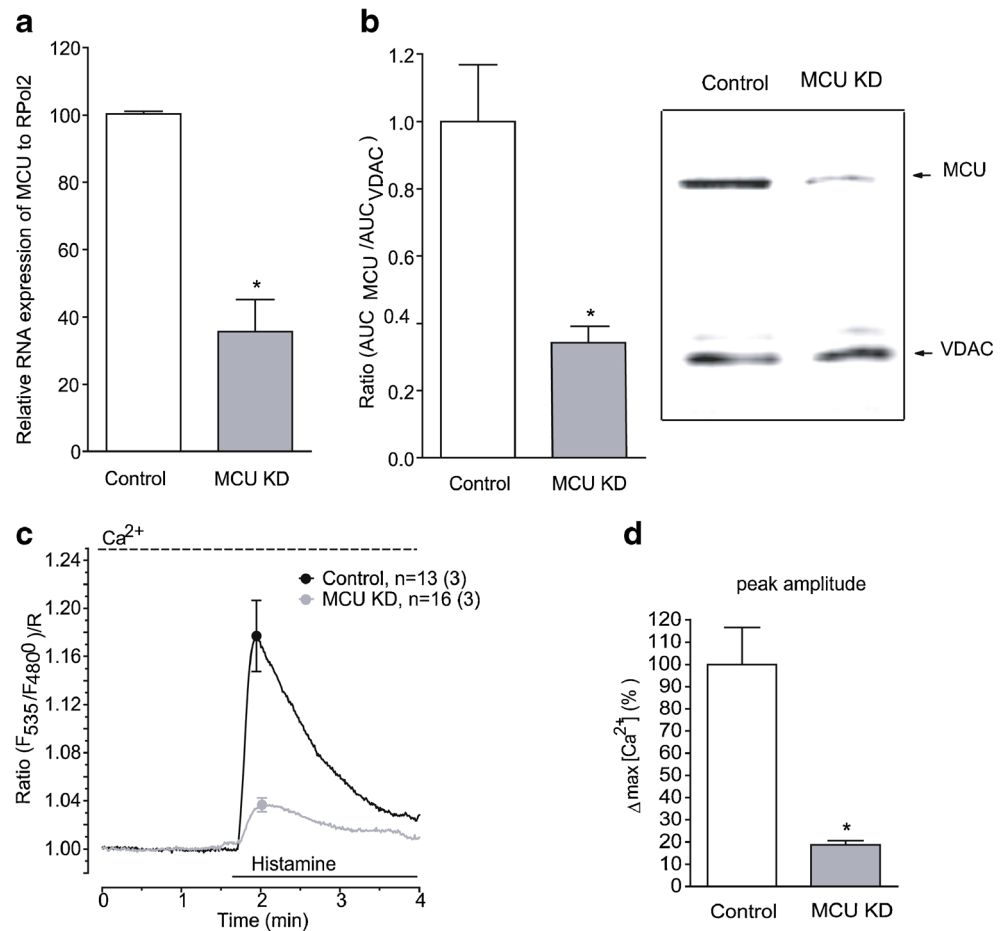
The occurrence probability was calculated as a fraction of patches displayed specific channel activity relative either to the total number of patches studied or the number of active patches displayed any type of the channel activity. Single channel analysis was performed using Clampfit 9.2 (Molecular Devices, Sunnyvale, CA, USA). Data are expressed as means with standard error. Statistical comparisons were conducted with a two-tailed unpaired *t* test. Values of *p* < 0.05 (\*) were taken as statistically significant. Statistical analysis was performed by Graph Pad Software version 5.01 (La Jolla, CA, USA).

## Results

### Stably knockdown of MCU strongly reduced mitochondrial Ca<sup>2+</sup> sequestration in intact HeLa cells

Diminution in MCU gene expression by stably expression of the respective shRNA in HeLa cells (MCU-KD cells) was confirmed by quantitative real-time PCR. In MCU-KD cells, the level of MCU mRNA expression was significantly depressed and amounted 36±10 % (*n*=3, *p*<0.005) of the level detected in control cells (Fig. 1a). Hence, Western blot analysis revealed that the cellular MCU protein content was attenuated to 33±6 % (*n*=2, *p*<0.08) of the level detected in control cells (Fig. 1b). In line with these findings, in MCU-KD cells, histamine-induced mitochondrial Ca<sup>2+</sup> elevation was reduced to 19 % of the level attained in control cells (Fig. 1c, d).

**Fig. 1** MCU knockdown impairs intramitochondrial  $\text{Ca}^{2+}$  rise during cell stimulation. **a** Relative RNA expression of control and MCU-KD cells, **b** MCU protein expression in control and MCU-KD cells. Representative bands for MCU and VDAC protein expression. **c** Averaged traces of mitochondrial  $\text{Ca}^{2+}$  signals upon stimulation with 100  $\mu\text{M}$  histamine of intact control HeLa cell (black trace,  $n=13$  cells from three coverslips) and MCU-KD HeLa cells (gray trace,  $n=16$  cells from three coverslips). Mitochondrial  $\text{Ca}^{2+}$  signals were measured using cells expressing 4mtD3cpv. **d** Quantitative expression of intramitochondrial  $\text{Ca}^{2+}$  rise during cell stimulation with 100  $\mu\text{M}$  histamine in MCU-KD cells relative to the rise in control cells



Knockdown of MCU strongly reduced whole-mitoplast  $\text{Ca}^{2+}$  currents

In whole-mitoplast configuration, switching from  $\text{Ca}^{2+}$ -free to  $\text{Ca}^{2+}$ -containing (3 mM) solution during voltage ramps from  $-160$  to  $+50$  mV resulted in an inward current at negative potentials (Fig.2a) that was sensitive to RuR (Fig.2b, c). In mitochondria isolated from MCU-KD cells, the current elicited by  $\text{Ca}^{2+}$  addition was strongly reduced (Fig.2d) to 17 % of the level attained in control cells, while it remained sensitive to RuR (Fig.2e, f). In control group, at  $-155$  mV, the  $\text{Ca}^{2+}$  current amplitude averaged  $-251.4 \pm 55.8$  pA ( $n=11$ ), while in mitoplasts isolated from MCU-KD cells, the current averaged  $-43.5 \pm 18.4$  pA ( $n=5$ ) (Fig.2g). These results are very similar to that published very recently by the group of Clapham [3] and demonstrate that diminution of MCU results in a pronounced suppression of RuR-sensitive transmitochondrial inward  $I_{\text{Ca}}$  accompanied by potent reduction of intramitochondrial  $\text{Ca}^{2+}$  rise in intact cells exposed to supramaximal concentrations of histamine (Fig.1c).

Diminution of MCU strongly reduced whole-mitoplast  $\text{Na}^{+}$  currents in the absence of  $\text{Ca}^{2+}$

In whole-mitoplast configuration, switching from  $\text{Na}^{+}$ -free to  $\text{Na}^{+}$ -containing divalent-free solution resulted in a development of a pronounced inward current at negative potentials (Fig.3a). The current amplitude was a function of the applied membrane voltage. A mean current amplitude at  $-155$  mV averaged  $706 \pm 142$  pA ( $n=8$ ). The current rapidly terminated upon removal of bath  $\text{Na}^{+}$  and was inhibited by 10  $\mu\text{M}$  RuR (Fig.3a–c). These observations indicate that in the absence of  $\text{Ca}^{2+}$ , external  $\text{Na}^{+}$  readily permeates the RuR-sensitive channel(s), and the amplitude of transmitochondrial  $\text{Na}^{+}$  current ( $I_{\text{Na}}$ ) is higher than that generated by  $\text{Ca}^{2+}$  influx, an observation that is in line with previous studies [7, 13].

Stable knockdown of MCU resulted in a marked suppression of whole-mitoplast inward  $\text{Na}^{+}$  current ( $I_{\text{Na}}$ ) elicited by voltage ramps to  $170.4 \pm 21.0$  pA ( $n=8$ ) that equals a reduction by 76 % (Fig.3d–g). These results demonstrate that MCU downregulation results in a pronounced suppression of transmitochondrial inward RuR-sensitive  $I_{\text{Na}}$ .

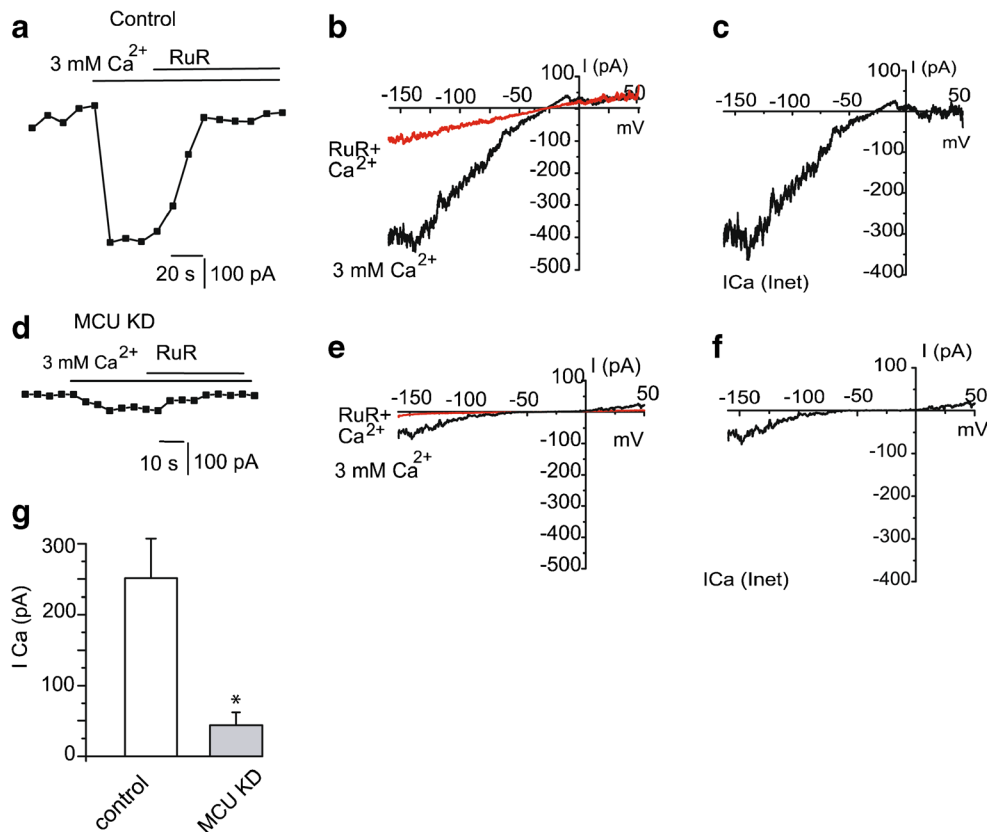


**Fig. 2** MCU knockdown suppresses whole-mitoplast  $\text{Ca}^{2+}$  current. **a** Exemplary time course of the whole-mitoplast current at  $-155$  mV before and after addition of  $3$  mM  $\text{Ca}^{2+}$  followed by addition of  $10$   $\mu\text{M}$  RuR ( $n=4$ ). Recording from mitoplast isolated from control cells. Voltage ramps were applied every  $10$  s. **b** Corresponding  $\text{Ca}^{2+}$  current responses to voltage ramps before and after addition of  $10$   $\mu\text{M}$  RuR in the presence of  $3$  mM  $\text{Ca}^{2+}$ . **c** Net  $I_{\text{Ca}}$  obtained after subtraction of RuR-insensitive current. **d** Representative time course of whole-mitoplast currents at

$-155$  mV induced by addition of  $3$  mM  $\text{Ca}^{2+}$  to the bath followed by addition of  $10$   $\mu\text{M}$  RuR. Recording from mitoplast isolated from MCU-KD cells. Voltage ramps were applied every  $5$  s. **e** Corresponding  $\text{Ca}^{2+}$  current responses to voltage ramps before and after addition of  $10$   $\mu\text{M}$  RuR in the presence of  $3$  mM  $\text{Ca}^{2+}$  ( $n=3$ ). **f** Net  $I_{\text{Ca}}$  obtained after subtraction of RuR-insensitive current. **g** Mean amplitudes of mitochondrial  $C_a$  from control ( $n=11$ ) and MCU-KD ( $n=5$ ) mitoplasts

Stable knockdown of MCU reduces the occurrence of active single channels per patch

We next characterized the probability of occurrence of any single channel activities of mitochondrial  $\text{Ca}^{2+}$  channels in the mitoplast-attached configuration [2] under conditions of MCU knockdown. Among 67 patches tested in mitochondrial from MCU-KD cells, only 35 patches displayed single channel activity, providing 52 % occurrence. In mitoplasts isolated from control cells, single channel activity was detected more frequently in 71 out of 103 patches tested, providing an occurrence probability of 69 %. For statistical processing, we analyzed the occurrence probability of the channel activity for each individual experimental day and calculated the mean values and statistics out of the individual values from all experimental days ( $N^D$ ). In the control group, the occurrence probability of single channel activities amounted  $71 \pm 6$  % ( $N^D=32$ ), while in MCU-KD group, the occurrence probability of single channel activities was

significantly ( $p < 0.05$ ) less and averaged  $47 \pm 8.0$  % ( $N^D=13$ ). Similar to mitoplasts from control group, in mitoplasts isolated from MCU-KD cells, we observed all three types of the channel activities described by us earlier [2].

Stable knockdown of MCU reduces the occurrence of *i*-MCC

We next analyzed the proportion of each individual channel activity in the total number of patches tested and to the number of active patches, which would give an indication on the density of individual channel type in the overall population of  $\text{Ca}^{2+}$  channels.

In mitochondria isolated from control cells, the most predominant channel was the  $11$  pS channel (intermediate conductance mitoplast  $\text{Ca}^{2+}$  channel, *i*-MCC) [2]. Exemplary traces of this type of activity in control and MCU-KD mitoplasts occasionally interrupted with bursting activity are depicted in Fig. 4a, b, respectively. Under control conditions, *i*-MCC activity was observed in 43 out of 103 patches tested



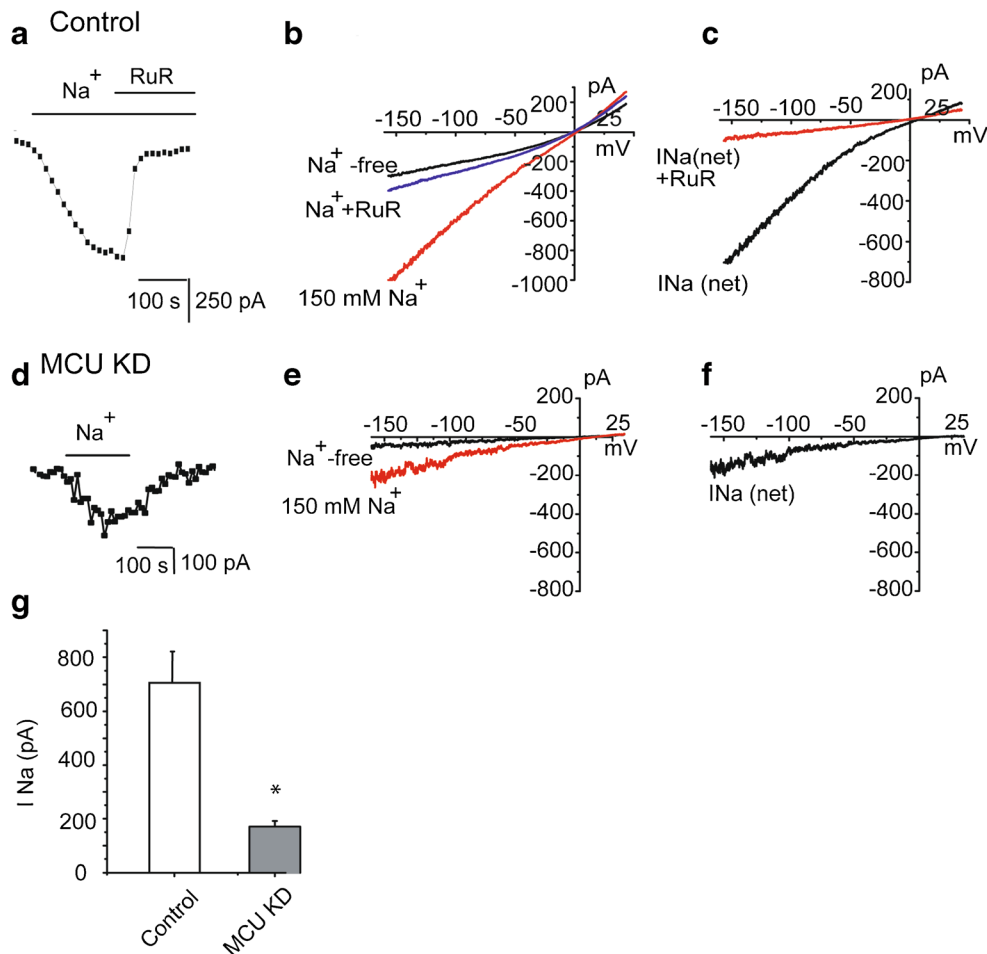


**Fig. 3** MCU knockdown suppresses whole-mitoplast  $\text{Na}^+$  current. **a** Exemplary time course of the whole-mitoplast current recorded from mitoplast isolated from control cells ( $n=8$ ) at  $-155$  mV. The current was elicited by replacement of bath TRIS for  $\text{Na}^+$  in divalent-free conditions and was measured during voltage ramps applied every 10 s. **b** Corresponding current responses to voltage ramps before ( $\text{Na}^+$  free) and after addition of 150 mM  $\text{Na}^+$  either alone or in the presence of 10  $\mu\text{M}$  RuR. **c** Net  $I_{\text{Na}(\text{Control})}$  obtained after subtraction of the background current obtained in  $\text{Na}^+$  and divalent-free solution. **d**

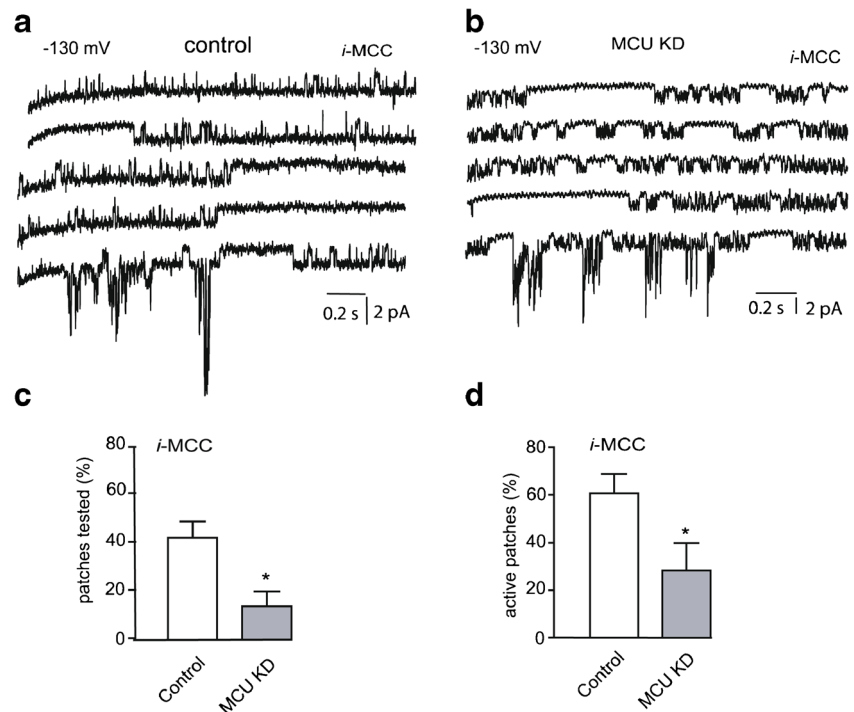
Representative time course of the whole-mitoplast current recorded from the mitoplast isolated from MCU-KD cells ( $n=8$ ) and measured at  $-155$  mV during voltage ramps applied every 10 s before and after replacement of bath TRIS for  $\text{Na}^+$  in divalent-free solution ( $n=8$ ). **e** Corresponding current responses to voltage ramps before ( $\text{Na}^+$  free) and after application of 150 mM  $\text{Na}^+$  to MCU-KD mitoplast. **f** Net  $I_{\text{Na}(\text{MCU-KD})}$  obtained after subtraction of background current. **g** Mean amplitudes of mitochondrial  $I_{\text{Na}}$  from control and MCU-KD groups

(occurrence probability  $42 \pm 7\%$ ,  $N^D=29$ ) (Fig.4c) and its individual contribution to active channels ( $n=71$ ) was  $61 \pm 8\%$  (Fig.4d). In mitochondria from MCU-KD cells, the occurrence probability of this channel was strongly reduced compared to controls: the *i*-MCC channel activity was detected in 11 out of 67 patches tested (occurrence probability  $14 \pm 6\%$ ,  $N^D=11$ ) (Fig.4c) and its individual contribution to active channels ( $n=35$ ) was  $28 \pm 12\%$  (Fig.4d). In MCU-KD group, the *i*-MCC conductance ( $11.5 \pm 0.5$  pS,  $n=6$ ) was not different from that observed in mitoplasts isolated from control cells ( $11.9 \pm 0.6$  pS,  $n=15$ ). Gating characteristics of *i*-MCC were slightly affected by MCU knockdown and revealed a tendency for reduced open probability (NPo) and mean open time ( $T_{o,\text{mean}}$ ) while mean closed time ( $T_{c,\text{mean}}$ ) was prolonged (Table 1).

Stable knockdown of MCU had no effect on the occurrence of the *b*-MCC

Similar to mitoplasts isolated from control cells (Fig.5a), the second type of the channel activity studied in mitoplasts isolated from MCU-KD cells was the bursting activity (Fig.5b). According to our previous reports, we refer to this channel as bursting mitochondrial  $\text{Ca}^{2+}$  channel (*b*-MCC) [2]. Neither occurrence nor conductance of *b*-MCC was altered in mitochondria isolated from MCU-KD cells. In control cells, this channel was observed in 23 out of 103 patches tested. The probability of occurrence of this channel activity was  $25 \pm 6\%$  ( $N^D=32$ ) in control group and  $23 \pm 9\%$  ( $N^D=13$ ) in the MCU-KD group in respect to all patches tested (Fig.5c). Within mitoplasts from MCU-KD cells, the *b*-MCC activity was

**Fig. 4** The occurrence probability of *i*-MCC channel is largely decreased in the inner mitochondria membrane from MCU-KD HeLa cells. **a** Representative single channel recording of *i*-MCC activity interrupted with *b*-MCC at a holding voltage of  $-130$  mV in mitoplast isolated from control cells. **b** Representative recording of *i*-MCC interrupted with *b*-MCC at a holding voltage of  $-130$  mV in mitoplast isolated from MCU-KD cells. **c** Bars represent the occurrence of *i*-MCC activity in mitoplasts from control and MCU-KD HeLa cells in respect to the total number of patches tested. **d** The same as in **c** but in respect to the number of active patches with any MCC activity



detected in 16 out of 67 patches tested (35 active patches) and the occurrence probability in respect to active patches was slightly higher ( $45 \pm 13$  %,  $N^D=11$ ) compared to the control group ( $33 \pm 7$  %,  $N^D=29$ ) (Fig.5d). In mitoplasts isolated from control cells, mean conductance of *b*-MCC channel was  $25.7 \pm 1.3$  pS ( $n=8$ ), and in MCU-KD mitoplasts, the channel conductance was unaltered and averaged  $26.0 \pm 1.8$  pS ( $n=9$ ) (Table 1).

Stable knockdown of MCU increased the occurrence of the *xl*-MCC

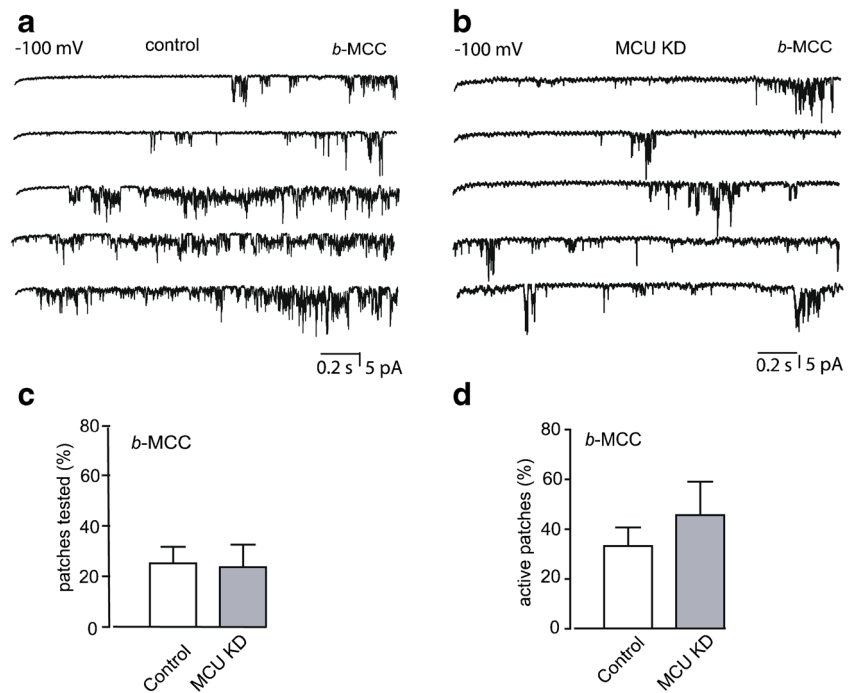
Both in control (Fig.6a) and MCU-KD group (Fig.6b), we also identified a third type of activity that we define as *xl*-MCC [2, 9]. In the control HeLa cells, *xl*-MCC conductance was  $74.8 \pm 7.9$  pS ( $n=8$ ), thus, comparable to that previously reported [2]. Diminution of MCU did not affect significantly

( $p > 0.05$ ) *xl*-MCC conductance  $70.7 \pm 5.9$  pS ( $n=6$ ) (Table 1). Remarkably, in the control group, this type of activity was the least frequent and was observed in 8 out of 103 patches tested, while in MCU-KD mitoplasts, this type of channel activity was observed in 10 out of 67 patches tested. The occurrence probability of this channel in respect to all patches studied was  $6 \pm 2$  % ( $N^D=32$ ) in the control group and  $13 \pm 5$  % ( $N^D=13$ ) in MCU-KD group, indicating a 2.3-fold increase in the occurrence probability of *xl*-MCC in MCU-KD mitoplasts (Fig.6c). When compared with respect to the number of active patches, the occurrence probability of *xl*-MCC in the MCU-KD group showed 4.3-fold increase from  $9 \pm 4$  % ( $N^D=29$ ) in the controls to  $38 \pm 14$  % ( $N^D=11$ ) in the MCU-KD group (Fig.6d). Gating characteristics of *xl*-MCC were also affected by MCU knockdown and revealed a significant reduction in  $NPo$ ,  $To_{mean}$ , while  $Tc_{mean}$  was not significantly altered (Table 1).

**Table 1** The effect of MCU knockdown on gating characteristics of mitochondrial  $Ca^{2+}$  currents (*i*-MCC and *xl*-MCC)

	Conductance (pS)	$NPo$	$To_{mean}$ (ms)	$Tc_{mean}$ (ms)	$n$
<i>i</i> -MCC control	$11.9 \pm 0.5$	$0.60 \pm 0.13$	$3.4 \pm 0.5$	$14.2 \pm 2.1$	15
<i>i</i> -MCC MCU-KD	$11.5 \pm 0.6$	$0.36 \pm 0.05$	$4.6 \pm 0.8$	$17.3 \pm 2.3$	6
<i>p</i> value	0.70	0.26	0.17	0.42	
<i>b</i> -MCC control	$25.7 \pm 1.3$	$0.39 \pm 0.08$	$2.7 \pm 0.4$	$27.7 \pm 4.9$	8
<i>b</i> -MCC MCU-KD	$26.0 \pm 1.8$	$0.40 \pm 0.13$	$1.6 \pm 0.3^*$	$12.5 \pm 2.6^*$	9
<i>p</i> value	0.89	0.98	0.04	0.01	
<i>xl</i> -MCC control	$74.8 \pm 7.9$	$0.74 \pm 0.08$	$31.2 \pm 5.0$	$50.0 \pm 14.4$	6
<i>xl</i> -MCC MCU-KD	$70.7 \pm 5.9$	$0.40 \pm 0.14^*$	$12.1 \pm 1.6^*$	$44.7 \pm 16.1$	6
<i>p</i> value	0.690	0.002	0.006	0.248	

**Fig. 5** MCU knockdown does not affect the occurrence probability of *b*-MCC. **a** Representative single channel recording of *b*-MCC activity at a holding voltage  $-100$  mV in mitoplast isolated from control cells. **b** Representative *b*-MCC recording from mitoplast isolated from MCU-KD HeLa cells. **c** Bars represent the occurrence of *b*-MCC activity in mitoplasts from control and MCU-KD HeLa cells in respect to the total number of patches. **d** The same as in **c** but in respect to the number of active patches with any MCC activity

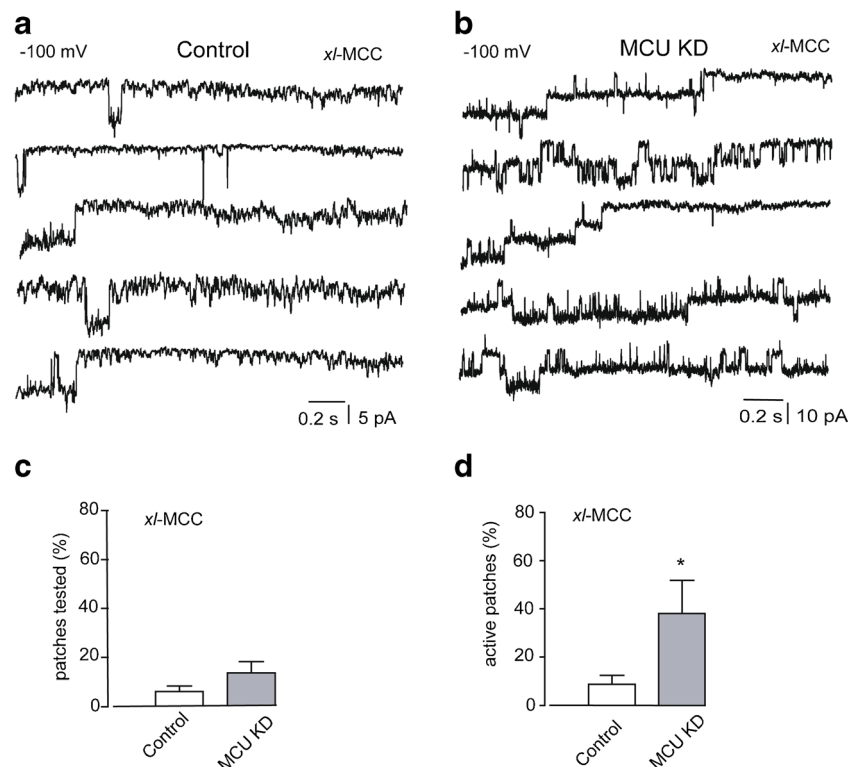


## Discussion

MCU has recently been identified as the ion-conducting pore in the mitochondrial inner membrane [1, 4]. However, several other studies have pointed for alternative putative channels/carriers for mitochondrial  $\text{Ca}^{2+}$  influx including mitochondrial

ryanodine receptors [20, 21], the  $\text{Ca}^{2+}/\text{H}^{+}$  antiporter leucine zipper EF hand-containing transmembrane protein 1 [10, 11, 25], the uncoupling proteins 2 and 3 [22, 23, 26], and the canonical transient receptor potential 3 channel [6]. Moreover, so far, two regulator proteins for mitochondrial  $\text{Ca}^{2+}$  uptake, the MICU1 [15, 18] and the MCUR1 [14], have been

**Fig. 6** Effect of MCU knockdown on the occurrence of *xl*-MCC activity. **a** and **b** Representative single channel recording of *xl*-MCC activity at a holding voltage  $-100$  mV in mitoplasts isolated from control (**a**) and MCU-KD cells (**b**). **c** Bars represent the occurrence of *xl*-MCC activity in mitoplasts from control and MCU-KD HeLa cells in respect to the total number of patches tested. **d** The same as in (**c**) but in respect to the number of active patches with any MCC activity





described, thus supporting the concept of a multiprotein complex being responsible to establish the mitochondrial  $\text{Ca}^{2+}$  uniporter phenomenon [8, 19]. While single channel measurements of mitochondrial  $\text{Ca}^{2+}$  channels in the mitoplast-attached configuration recently confirmed the existence of multiple mitochondrial  $\text{Ca}^{2+}$  entry pathways [2, 9, 17, 21], the actual proteins that account for the individual channels are unknown. Therefore, in the present study, we explored the effect of MCU knockdown on the occurrence probability of distinct types of single channel activities in the inner mitochondria membrane of HeLa cells and the amplitude of whole-mitoplast inward  $\text{Ca}^{2+}$  and  $\text{Na}^+$  currents.

In whole-mitoplast configuration, diminution of MCU considerably reduced the inward  $\text{Ca}^{2+}$  current, an observation similar to that published previously [3]. Applying voltage ramps in divalent-free conditions produced a development of a linear inward current upon switching from  $\text{Na}^+$ -free to  $\text{Na}^+$ -containing solution. The current was sensitive to ruthenium red and had higher amplitude than the current developed when  $\text{Ca}^{2+}$  was added to the bath in the absence of  $\text{Na}^+$ , indicating that in the absence of  $\text{Ca}^{2+}$ , the channels permeate  $\text{Na}^+$ , an observation consistent with the previous ones [7, 13]. We used this intrinsic property of mitochondrial  $\text{Ca}^{2+}$  permeable channel(s) to better discriminate the consequences of MCU silencing on electrical signaling of mitoplasts. Here, we show that MCU knockdown effectively suppresses transmitochondrial currents carried by  $\text{Ca}^{2+}$  and  $\text{Na}^+$ . The degree of  $I_{\text{Ca}}$  and  $I_{\text{Na}}$  suppression upon MCU knockdown corresponded well to the degree of suppression of mitochondrial  $\text{Ca}^{2+}$  accumulation in intact cells upon histamine exposure. These findings confirm a very recent report that describes a large reduction of ruthenium red-sensitive whole-mitoplast currents of HEK293 cells with RNAi-mediated knockdown of the MCU [3].

In addition to the evaluation on the knockdown of MCU on ruthenium red-sensitive whole-mitoplast currents, we also explored whether MCU knockdown affects the occurrence probability of the individual and distinct single channel activities previously reported in HeLa mitoplast [2]. We found that the occurrence probability of active patches has been largely reduced in MCU-KD mitoplasts, thus supporting the concept of MCU being the main conducting pore of mitochondrial  $\text{Ca}^{2+}$  currents. However, we found that this reduction is mostly due to reduced occurrence probability of *i*-MCC channel that represents one (i.e., *i*-MCC; app. 14.3 pS) [9] out of three  $\text{Ca}^{2+}$  currents (*i*-MCC, *b*-MCC, and *xl*-MCC) in mitoplasts isolated from HeLa cells [2]. Although it was shown that purified MCU shows channel activity in lipid bilayers where under symmetrical 100 mM  $\text{Ca}^{2+}$  conditions the channel conductance was reported to be 6–7 pS [4], one can speculate that in its natural environment and under asymmetrical  $\text{Ca}^{2+}$  conditions, the MCU conductance may differ, possibly due to the formation of hetero-multimers. This

assumption is in line with other reports on native mitoplasts isolated from cardiac myocytes and endothelial cells where two different channels with the conductance of app. 13–14 and 7–8 pS have been discriminated under asymmetrical  $\text{Ca}^{2+}$  conditions [9, 17]. Accordingly, the selective decrease in occurrence probability of *i*-MCC upon MCU knockdown observed in the present study suggests that this type of activity is indicative for the MCU-established current.

The other observation of the present study is that MCU knockdown yielded an increased occurrence probability of *xl*-MCC channel activity in respect to active channels. This observation indicates that *xl*-MCC (app. 74–77 pS) [2, 9] is independent from the presence of MCU protein and mitochondrial  $\text{Ca}^{2+}$  channels other than MCU play a compensatory role under functional MCU diminution. Notably, our statistical analysis regarding the individual gating characteristics of *i*-MCC and *xl*-MCC revealed a decrease in the mean NPo and  $T_{\text{mean}}$  of both channels in mitoplasts from MCU-KD cells. However, in view of the rather large variances in these measurements, caution is necessary in the interpretation of these changes. Nevertheless, these data further support the concept of a rather complex mitochondrial  $\text{Ca}^{2+}$  uptake machinery that might consist from MCU-dependent and MCU-independent pathways that are functionally interrelated to meet the versatile  $\text{Ca}^{2+}$  demand of the organelle under different conditions of high and low metabolic and ion fluxes.

It is still unclear whether *b*-MCC and *xl*-MCC represent distinct or the same channel protein. However, because of observation that *b*-MCC could turn into *xl*-MCC activity, it is reasonable to suggest that a single channel pore protein accomplishes two distinct activities. Because the pipette solution for single channel recordings in the present study contained CGP37157, an inhibitor of  $\text{NCX}_{\text{mito}}$ , which partially inhibits pH-dependent  $\text{Ca}^{2+}$  transport (Letm1), and because *xl*-MCC is a channel, mitochondrial  $\text{Na}^+/\text{Ca}^{2+}$  exchanger(s) and Letm1 can be excluded from being responsible for *xl*-MCC current. Thus, further studies are needed to identify the molecular player(s) governing the *xl*-MCC activity.

Overall, the present study addressed the role of MCU in transmitochondrial  $\text{Ca}^{2+}$  fluxes using the direct patch-clamp approach on mitoplasts isolated from HeLa cells with diminished MCU expression and respective controls. Our current study shows that MCU knockdown results in a strong decrease in whole-mitoplast current and the number of active patches with  $\text{Ca}^{2+}$  channel behavior. Notably, this decrease is exclusively due to a decrease in the number of active recently identified *i*-MCC but not *b*-MCC or *xl*-MCC of which the latter one seems to play a compensatory role under conditions of MCU knockdown. Nevertheless, as gating characteristics for *i*-MCC and *xl*-MCC were affected by diminution of MCU, our findings point to a modulatory interaction between

the two independent  $\text{Ca}^{2+}$  currents the nature of which awaits to be identified.

**Acknowledgments** We thank Rene Rost, PhD. for his excellent technical assistance. This work was supported by the Austrian Science Funds (FWF, P20181-B05 P21857-B18 and P22553-B18). C.J.-Q. is a fellow of the Doctoral College “Metabolic and Cardiovascular Disease” funded by the Austrian Science Fund (W1226-B18) and the Medical University of Graz, the University of Graz and the Graz University of Technology. W.P. is supported by the Austrian academic exchange services (ÖAD).

**Open Access** This article is distributed under the terms of the Creative Commons Attribution License which permits any use, distribution, and reproduction in any medium, provided the original author(s) and the source are credited.

## References

- Baughman JM, Perocchi F, Girgis HS, Plovianich M, Belcher-Timme CA, Sancak Y, Bao XR, Strittmatter L, Goldberger O, Bogorad RL, Kotliansky V, Mootha VK (2011) Integrative genomics identifies MCU as an essential component of the mitochondrial calcium uniporter. *Nature* 476:341–345
- Bondarenko AI, Jean-Quartier C, Malli R, Graier WF (2013) Characterization of distinct single-channel properties of  $\text{Ca}^{2+}$  inward currents in mitochondria. *Pflugers Arch* 465:997–1010
- Chaudhuri D, Sancak Y, Mootha VK, Clapham DE (2013) MCU encodes the pore conducting mitochondrial calcium currents. *eLife* 2: e00704–e00704
- De Stefani D, Raffaello A, Teardo E, Szabò I, Rizzuto R (2011) A forty-kilodalton protein of the inner membrane is the mitochondrial calcium uniporter. *Nature* 476:336–340
- Duchen MR (2000) Mitochondria and  $\text{Ca}^{2+}$  in cell physiology and pathophysiology. *Cell Calcium* 28:339–348
- Feng S, Li H, Tai Y, Huang J, Su Y, Abramowitz J, Zhu MX, Birnbaumer L, Wang Y (2013) Canonical transient receptor potential 3 channels regulate mitochondrial calcium uptake. *Proc Natl Acad Sci U S A* 110:11011–11016
- Fieni F, Bae Lee S, Jan YN, Kirichok Y (2012) Activity of the mitochondrial calcium uniporter varies greatly between tissues. *Nat Comms* 3:1317
- Graier WF, Frieden M, Malli R (2007) Mitochondria and  $\text{Ca}^{2+}$  signaling: old guests, new functions. *Pflugers Arch* 455:375–396
- Jean-Quartier C, Bondarenko AI, Alam MR, Trenker M, Waldeck-Weiermair M, Malli R, Graier WF (2012) Studying mitochondrial  $\text{Ca}^{2+}$  uptake—a revisit. *Mol Cell Endocrinol* 353:114–127
- Jiang D, Zhao L, Clapham DE (2009) Genome-wide RNAi screen identifies Letm1 as a mitochondrial  $\text{Ca}^{2+}/\text{H}^{+}$  antiporter. *Science* 326: 144–147
- Jiang D, Zhao L, Clish CB, Clapham DE (2013) Letm1, the mitochondrial  $\text{Ca}^{2+}/\text{H}^{+}$  antiporter, is essential for normal glucose metabolism and alters brain function in Wolf-Hirschhorn syndrome. *Proc Natl Acad Sci U S A* 110:E2249–E2254
- Kim I, Yang D, Tang X, Carroll JL (2011) Reference gene validation for qPCR in rat carotid body during postnatal development. *BMC Res Notes* 4:440
- Kirichok Y, Krapivinsky G, Clapham DE (2004) The mitochondrial calcium uniporter is a highly selective ion channel. *Nature* 427:360–364
- Mallilankaraman K, Cárdenas C, Doonan PJ, Chandramoorthy HC, Irrinki KM, Golenár T, Csordás G, Madireddi P, Yang J, Müller M, Miller R, Kolesar JE, Molgó J, Kaufman B, Hajnóczky G, Foskett JK, Madesh M (2012) MCU1 is an essential component of mitochondrial  $\text{Ca}^{2+}$  uptake that regulates cellular metabolism. *Nat Cell Biol* 14:1336–1343
- Mallilankaraman K, Doonan P, Cárdenas C, Chandramoorthy HC, Müller M, Miller R, Hoffman NE, Gandhirajan RK, Molgó J, Binbaum MJ, Rothberg BS, Mak D-OD, Foskett JK, Madesh M (2012) MICU1 is an essential gatekeeper for MCU-mediated mitochondrial  $\text{Ca}^{2+}$  uptake that regulates cell survival. *Cell* 151: 630–644
- Mehta R, Birerdinc A, Hossain N, Afendy A, Chandhoke V, Younossi Z, Baranova A (2010) Validation of endogenous reference genes for qRT-PCR analysis of human visceral adipose samples. *BMC Mol Biol* 11:39
- Michels G, Khan IF, Endres-Becker J, Rottlaender D, Herzig S, Ruhparwar A, Wahlers T, Hoppe UC (2009) Regulation of the human cardiac mitochondrial  $\text{Ca}^{2+}$  uptake by 2 different voltage-gated  $\text{Ca}^{2+}$  channels. *Circulation* 119:2435–2443
- Perocchi F, Gohil VM, Girgis HS, Bao XR, McCombs JE, Palmer AE, Mootha VK (2010) MICU1 encodes a mitochondrial EF hand protein required for  $\text{Ca}^{2+}$  uptake. *Nature* 467:291–296
- Pizzo P, Drago I, Filadi R, Pozzan T (2012) Mitochondrial  $\text{Ca}^{2+}$  homeostasis: mechanism, role, and tissue specificities. *Pflugers Arch* 464:3–17
- Ryu SY, Beutner G, Dirksen RT, Kinnally KW, Sheu S-S (2010) Mitochondrial ryanodine receptors and other mitochondrial  $\text{Ca}^{2+}$  permeable channels. *FEBS Lett* 584:1948–1955
- Ryu SY, Beutner G, Kinnally KW, Dirksen RT, Sheu S-S (2011) Single channel characterization of the mitochondrial ryanodine receptor in heart mitochondria. *J Biol Chem* 286:21324–21329
- Trenker M, Fertschai I, Malli R, Graier WF (2008) UCP2/3 - likely to be fundamental for mitochondrial  $\text{Ca}^{2+}$  uniport. *Nat Cell Biol* 10: 1237–1240
- Trenker M, Malli R, Fertschai I, Levak-Frank S, Graier WF (2007) Uncoupling proteins 2 and 3 are fundamental for mitochondrial  $\text{Ca}^{2+}$  uniport. *Nat Cell Biol* 9:445–452
- Waldeck-Weiermair M, Deak AT, Groschner LN, Alam MR, Jean-Quartier C, Malli R, Graier WF (2013) Molecularly distinct routes of mitochondrial  $\text{Ca}^{2+}$  uptake are activated depending on the activity of the sarco/endoplasmic reticulum  $\text{Ca}^{2+}$  ATPase (SERCA). *J Biol Chem* 288:15367–15379
- Waldeck-Weiermair M, Jean-Quartier C, Rost R, Khan MJ, Vishnu N, Bondarenko AI, Imamura H, Malli R, Graier WF (2011) The leucine zipper EF hand-containing transmembrane protein 1 (LETM1) and uncoupling proteins- 2 and 3 (UCP2/3) contribute to two distinct mitochondrial  $\text{Ca}^{2+}$  uptake pathways. *J Biol Chem* 286: 28444–28455
- Waldeck-Weiermair M, Malli R, Naghdi S, Trenker M, Kahn MJ, Graier WF (2010) The contribution of UCP2 and UCP3 to mitochondrial  $\text{Ca}^{2+}$  uptake is differentially determined by the source of supplied  $\text{Ca}^{2+}$ . *Cell Calcium* 47:433–440